3. Results

3.1 Generation of *Tshz1* and *Tshz2* mutant mice

In order to investigate *Tshz1* and *Tshz2* functions in mouse development, I designed two targeting strategies aiming to introduce null alleles for these genes into the mouse genome through homologous recombination in ES cells. Both *Tshz1* and *Tshz2* consist of a first small exon and a second large one (about 4 Kb), which contains the whole protein coding sequence. Therefore, I disrupted in both cases exon 2 through the insertion of a GFP cassette. Since *Tshz1* knock out mice were found to be not viable and to die about ten hours after birth, I later designed a targeting strategy aimed to mutate the *Tshz1* exon 2 conditionally.

3.1.1 Isolation of BAC – clones for *Tshz1* and *Tshz2*

A DNA probe for each gene was PCR - amplified from genomic DNA and used to screen a BAC–library from the mouse genome, derived from 129/SvEvTac mice. Three BAC–clones containing *Tshz1* and six containing *Tshz2* were isolated. The integrity of the *Tshz* sequences in these clones was verified through further Southern Blot hybridizations with different probes.

3.1.2 Generation of *Tshz1* knock out mice and of *Tshz1* floxed allele

Establishment of Tshz1 genomic subclone

One of the BAC clones containing *Tshz1* was used as a starting point for the generation of a targeting vector. A fragment of *Tshz1* genomic sequence was isolated from it through homologous recombination in bacteria. To achieve this, I modified a DNA fragment containing the sequence of the vector pBluescript II and a cassette for negative selection in ES cells. At both ends of the DNA fragment a sequence homologous to that of the *Tshz1* locus was placed, to allow the recombination (Fig. 3.0). This way, a 15 kb fragment of the *Tshz1* locus containing exon2 was isolated, and used to construct the targeting vectors both for the knock out allele and the conditional allele. This subclone was flanked by a cassette that contains the sequence for Diphtheria Toxin A (DTA) and that later served as a negative selectable marker. In case of random integration in the mouse genome during recombination in ES cells, the resulting expression of DTA protein would lead to cell death.

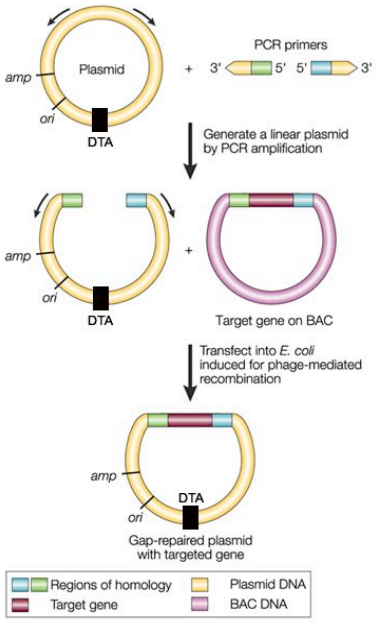

Fig.3.0. A mouse genomic DNA fragment of 15kb was retrieved from bacterial artificial cromosome (BAC) into a PCR-amplified vector containing the DTA cassette for negative selection. For this, the vector was PCR-amplified using primers that contained region of homology to the genomic fragment to subclone, and subsequently it was transformed into recombinant-competent cells containing the BAC. Recombination occurs between homologies at the end of the vector and the BAC DNA. (Figure adapted from Copeland et al., 2001)

Establishment of a targeting vector for the generation of Tshz1 reporter allele

In order to construct a targeting vector to delete *Tshz1* from the mouse genome, I replaced in the 15 kb subclone almost the entire *Tshz1* coding sequences by Gap43–GFP coding sequences (Fig.3.1A). The *Tshz1* start codon and the sequence coding for the first three amino acids of the *Tshz1* protein were maintained and fused to the start codon of the Gap43-GFP coding sequence. The nucleotides forming the start codon were exchanged to fit to the Kozac–sequence (GCCRCCATGG, R = A or G), which enhances translation in vertebrates (Kozac, 1987). The Gap43–GFP cassette consists of the sequence coding for the N-terminal peptide of the membrane-anchored Neuromodulin Gap43, fused with the GFP coding sequence; the GFP–fusion protein is therefore anchored to the cell membrane. In mice bearing the Gap43–GFP reporter allele, it is possible to identify the cells where *Tshz1* is expressed through the visualization of GFP. Next to the Gap43–GFP reporter gene, the targeting vector contained the neomycin–resistance gene, which was flanked by two loxP sites. The Neo–cassette allowed the selection of the ES cell clones in which the targeting vector was integrated; as the resistance cassette can have unpredictable consequences in vivo, such as misregulation of adjacent genes or the attenuation of expression of the gene of interest, its elimination from the mouse genome was desirable. For this purpose, I included in the vector a "self excision" cassette under the control of a specific testis promotor, which encodes the gene Cre–recombinase. The

Cre–recombinase recognizes the loxP sequences and excises through recombination the DNA fragment localized between the loxP sites; its expression is driven by a testis-specific promoter, so that the Neo–cassette survives selection in cultured cells, but is removed along with Cre as they both are passed through the male germline (Bunting et al., 1999). Finally, a poly –A sequence was inserted at the 3´end of the cassette.

Establishment of a targeting vector for the generation of Tsh1^{flox} allele

Since *Tshz1* knockout mice were not viable, I designed a targeting strategy that intended to mutate the gene conditionally, in order to allow *Tshz1* inactivation in a tissue specific manner (Fig.3.1B). To achieve this, a targeting vector was constructed in which exon 2, which contains the entire coding sequence for *Tshz1* protein, was flanked by loxP sites. Upon expression of Cre recombinase, the exon is deleted and *Tshz1* protein is not produced from the mutant allele. The loxP sites should not interfere with the function of the floxed gene and therefore they were inserted in intron sequences that are not highly conserved among species.

The starting point for the construction of the targeting vector was again the 15 kb subclone isolated from one of the BAC clones containing *Tshz1*. Two cassettes were inserted, the first upstream and the second downstream of exon 2. The 5´cassette contained the first loxP site; moreover, it contained a Neo-resistance cassette, for the selection of the positive ES cell clones, flanked by two FRT sites. After selection and isolation of the positive ES cells clones, the Neo–cassette would be excised through homologous recombination of the FRT sites, after expression of a Flp recombinase in the mouse germline. The 3´cassette contained the second loxP and an additional EcoRI site necessary for the screening of the ES cell clones by Southern Blot. The correct orientation of loxP sites was confirmed by cre–mediated recombination of the "floxed" sequences in bacteria.

Mutation of Tshz1 locus in ES-cells

The targeting vectors were linearized using Pac I site and were then electroporated into E14.1/129 Ola ES cells (Thomas and Capecchi, 1987; Mansour et al., 1988; Kühn et al., 1991). The *Tshz1*^{flox} targeting vector was also electroporated into R1/129 SV ES cells (Rossant and Nagy, 1995); I electroporated the floxed vector into two

different ES cell lines to increase the probability of integration in the genome since I did not obtain homologous recombination in E14.1/129 Ola ES cells. Possible differences between sequences from the two ES cell lines, which are derived from different inbred mouse strains might have affected the homologous recombination frequencies of the targeting vector that derived from 129/SvEvTac genomic DNA.
Two days after electroporation, ES cells were selected with the antibiotic G418 (geneticin) for the presence of the *neomycin* resistance gene. A total of 400 colonies for each electroporation were picked and expanded; one aliquot of each clone was then frozen for storage, and another was used for the isolation of genomic DNA. Southern hybridization was used to detect homologous recombination events, and the insertion of a single vector was verified. For this, external and internal probes derived from the *Tshz1* locus were used (Fig.3.2).
In the case of *Tshz1*^{GFP} electroporation, out of 250 screened ES cell clones 9 had inserted the vector by homologous recombination, i.e. the recombination efficiency was 3.6%. As for the *Tshz1*^{flox} electroporation in E14.5/129 Ola ES cells, 300 clones were screened, but none showed homologous recombination. Differently, in the case of the electroporation in R1/RV Ola ES cells, 17 positive clones were found among 200 screened (recombination efficiency 8.5%). (Fig. 3.2)

Three independent *Tshz1*^{GFP} +/- ES cell clones were injected into C57BL/6 blastocysts and transferred into foster mothers. The injections were performed in the transgenic core facility of the MDC. From injected blastocysts, several chimeric mice developed, and three males from each ES cell clone were chosen and backcrossed to C57BL/6 females. Brown offspring were identified, and germ line transmission of the *Tshz1*^{GFP} allele was confirmed by Southern blot analysis (Fig.3.3.). Heterozygous mice (F1) were then crossed to obtain homozygous *Tshz1*^{GFP} mice. Homozygous *Tshz1*^{GFP} mice didn't survive more than 10 – 12 hours after birth. They showed breathing difficulties and in most cases a swollen abdomen because of an accumulation of air in the intestine (Fig.3.3). The cause of postnatal death is not known.

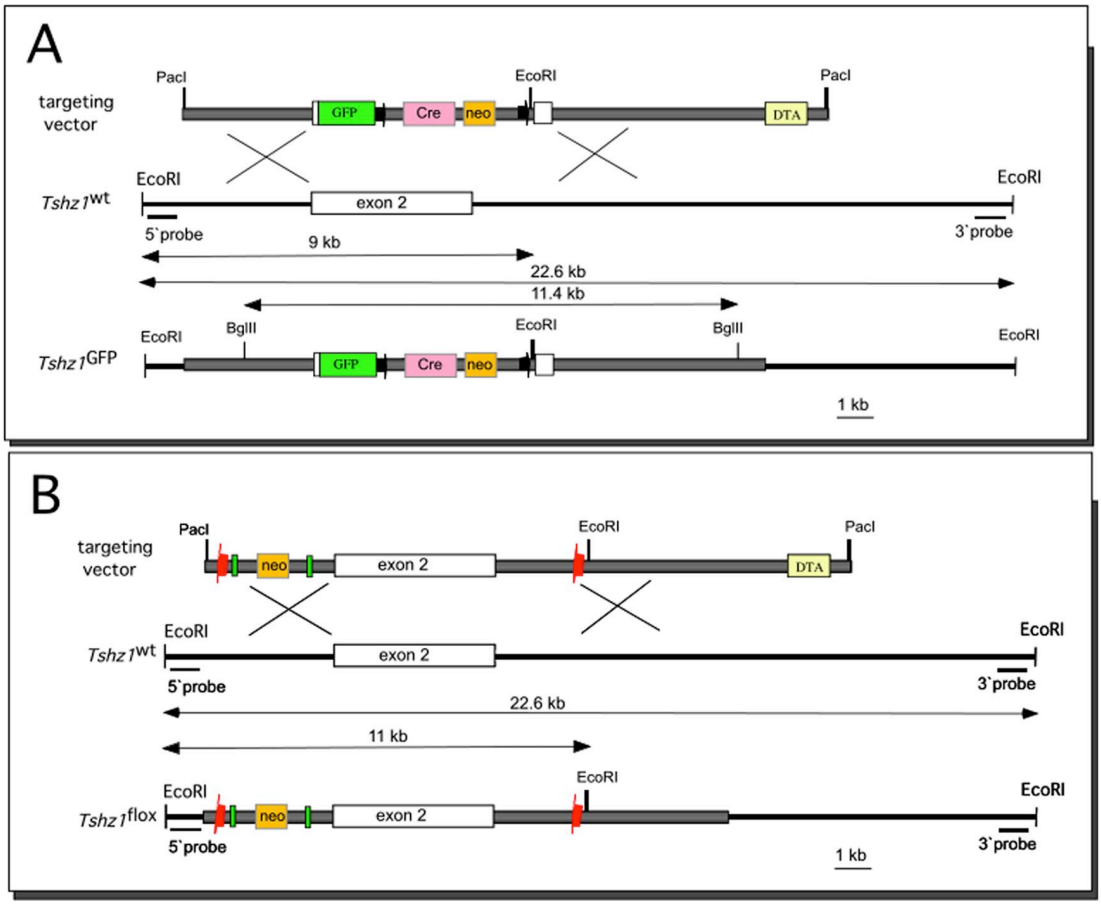

Fig.3.1. Strategies for *Tshz1* mutation. (A) Schematic representation of the targeting strategy employed to generate the *Tshz1*^{GFP} allele. The *Tshz1* genomic locus, where exon2 is represented by a white box, is shown; moreover, targeting vector and targeted locus containing the GFP coding sequence (green), Cre-recombinase (pink), neomycin-resistance gene (orange) and DTA (yellow) are shown. EcoRI and BglII restriction sites are indicated. (B) Targeting strategy used to generate the *Tshz1*^{flox} allele. The loxP sites (shown as arrowheads) flank exon2 and the neomycin resistance gene. Neomycine casette is flanked by FRT sites (green). The probes used for Southern blot analysis, as well as the predicted size of DNA fragments obtained after EcoRI digestion, are indicated.

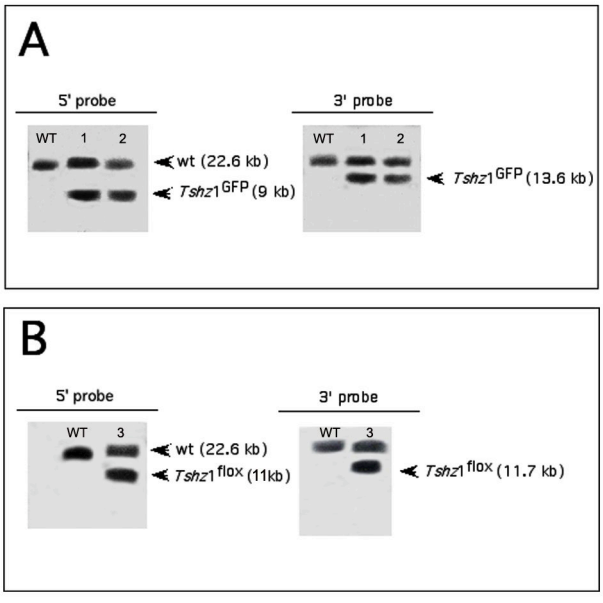

Fig.3.2. Southern blot-analysis of ES cell DNA after EcoR1 digestion. The hybridization was performed with two external probes, 3´and 5´. (A) WT and *Tshz1*$^{GFP/+}$ ES cell clones 1 and 2; the *Tshz1*^{GFP} allele was identified by 9kb (5') and 13.6kb (3') hybridization bands. (B) WT and *Tshz1*$^{flox/+}$ ES cell clone 3; the *Tshz1*^{flox} allele was identified by 11kb (5') and 11.7 kb (3') hybridization bands.

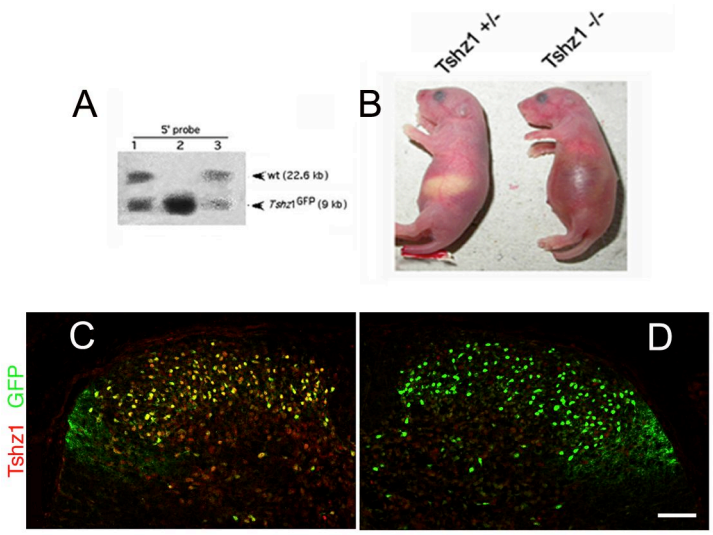

Fig.3.3 (A) Southern blot analysis of EcoRI digested genomic DNA from *Tshz1*$^{GFP/+}$ (lane1) and *Tshz1*$^{GFP/GFP}$ (lane2) mice and *Tshz1*$^{GFP/+}$ ES cell clone (lane3). (B) Control (left) and *Tshz1*$^{GFP/GFP}$ (right) mice five hours after birth. Immunohystological analysis of spinal cord coronal section of *Tshz1*$^{GFP/+}$ (C) and *Tshz1*$^{GFP/GFP}$ (D) E18.0 mice stained with anti-*Tshz1* (red) and anti-GFP (green) antibodies. Bar. 500μm.

3.1.3 Generation of *Tshz2* knock out mice

Establishment of Tshz2 genomic subclone

As already described for *Tshz1*, for the targeting of the *Tshz2* locus the starting point was the isolation of a genomic subclone from one of the *Tshz2*-containing BAC clones. A 16kb subclone was recombined into a DNA fragment containing the sequence of the vector pBluescript II and the DTA cassette for negative selection in ES cells. This construct was used as a starting point to create the targeting vector for the knock out allele.

Establishment of a targeting vector for the generation of Tshz2 reporter allele

In the 16kb subclone, the *Tshz2* reading frame was almost entirely substituted with the Gap43-GFP coding sequence (Fig.3.4 A). As described above for *Tshz1*, the starting codon and the sequence coding for the first 3 amino acids were maintained and fused to the starting codon of the Gap43-GFP coding sequence. Also in this case, the starting codon was Kozak–optimized. Next to the Gap43-GFP reporter gene, the

targeting vector contained the "self excision" neomycin–resistance cassette, as well as a poly–A sequence.

Mutation of Tshz2 locus in ES-cells

The targeting vector was linearized using the PmeI site and was then electroporated into E14.5/129 Ola ES cells (Thomas and Capecchi, 1987; Mansour et al., 1988). Two days after electroporation ES cells were selected with antibiotic G418 for the presence of the *neomycin* resistance gene. 400 resistant colonies were picked, expanded and split into two aliquots, one of which was frozen for storage, and the other was used for the isolation of genomic DNA. Southern hybridization screening with external and internal probes allowed to detect 5 clones in which the vector was correctly inserted, out of 250 clones screened (recombination efficiency 2%). (Fig. 3.4).

Three independent *Tshz2*^{GFP} +/- ES cell clones were injected into C57BL/6 blastocysts and transferred into foster mothers. From three injections, several chimeric mice were obtained and backcrossed to C57BL/6 females. Germ line transmission of the *Tshz2*^{GFP} allele to brown offspring was confirmed by Southern blot analysis (Fig.3.4 B). F1 mice were then crossed to obtain homozygous *Tshz2*$^{GFP/GFP}$ mice. Homozygous *Tshz2*$^{GFP/GFP}$ mice were viable, fertile and have a normal life span; during postnatal life, they were smaller in size than wild type animals, but during adulthood the difference disappears and the mutants became indistinguishable from the controls.

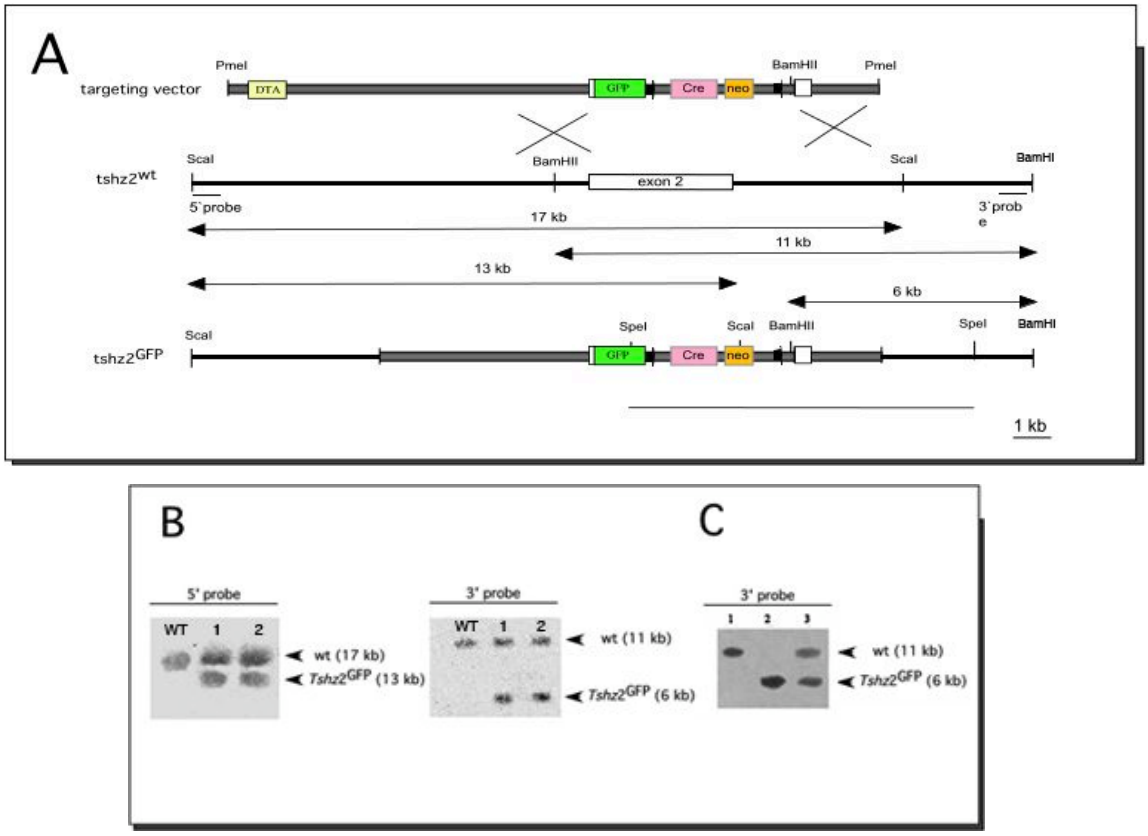

Fig.3.4. Generation of *Tshz2* knock out mice. (A) Schematic representation of the targeting strategy employed to generate the *Tshz2*^{GFP} allele. Exon 2, containing the open reading frame, is indicated as a white box. The GFP coding sequence (green), the *Cre*-recombinase (pink), the *Neomycin*-cassette (orange) and the DTA-cassette (yellow) are shown. ScaI, BamHI and SpeI sites are indicated. **(B)** Southern Blot analysis from WT and *Tshz2*$^{GFP/+}$ ES cell clones 1 and 2. The hybridization was performed with two external probes, 3´ (hybridized to BamHI digested ES cell DNA) and 5´ (hybridized to ScaI digested ES cell DNA). The Tshz2^{GFP} allele was identified by 13kb (5') and 6kb (3') hybridization bands. **(C)** Southern blot analysis of BamHI digested genomic DNA from wild type (lane1) and *Tshz2*$^{GFP/GFP}$ (lane 2) mice and *Tshz2*$^{GFP/+}$ ES cell clone (lane3).

3.2 Analysis of *Teashirt* gene expression in murine developing spinal cord

The three murine *Teashirt* genes were identified amongst more than one hundred genes with enriched expression in the dorsal spinal cord of the postnatal mouse, using an Affymetrix microarray hybridization screening. This work was undertaken by Dr. A. Garratt in order to identify genes with a potential function in the development and maturation of the dorsal spinal cord. The *Teashirt* genes were further selected for functional analysis in the mouse.

I analyzed the mRNA distribution of the three *Teashirt* genes in the developing spinal cord through in situ-hybridization at different embryonic stages (Fig.3.5). The expression patterns of *Tshz1*, *Tshz2* and *Tshz3* were distinct at early developmental stages, while at late gestation they partially overlapped and were restricted to the dorsal spinal cord. At E10.5 *Tshz1* was strongly expressed in the dorso–lateral spinal cord; *Tshz2* was only detected in the ventral spinal cord, while *Tshz3* expression was very weak and limited to the superficial part of the dorsal spinal cord. At E12.5 *Tshz1* transcripts were detected in several regions of the dorsal spinal cord, while *Tshz2* has broader expression and was also found in discrete neuronal subpopulations in the ventral spinal cord. Expression of *Tshz3* is limited to the dorsal spinal cord. At E14.5 *Tshz1* and *Tshz2* expression were broad and extended to ventral regions of the spinal cord, while *Tshz3* expression remained restricted to the very dorsal domain.

From E16.5 onwards, the expression patterns of the three genes became restricted to layers of the dorsal spinal cord. Interestingly, at E16.5 *Tshz1* and *Tshz2* marked selectively complementary layers in the dorsal spinal cord, while Tshz3 mRNA was more uniformly distributed. The layer specificity was maintained in postnatal life, as shown in Fig. 3.6, where Tshz1 immunoreactivity is confined to the most superficial layer of the spinal cord, while Tshz2 expands to deeper layers. Nevertheless, most of the Tshz1 positive cells are also Tshz2 positive, suggesting a possible functional collaboration or redundancy of the two transcription factors.

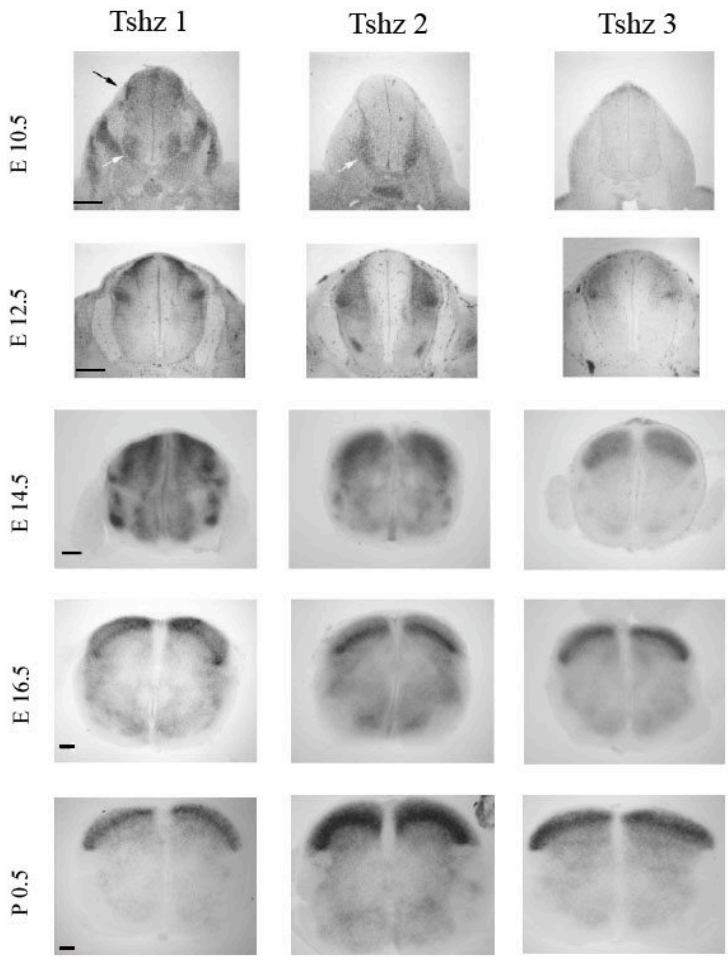

Fig 3.5. In situ hybridization analysis of mouse *Teashirt* expression in the spinal cord. Transverse sections of E10.5, E12.5, E14.5, E16.5 and P0.5 spinal cords were hybridized with *Tshz1* (lane 1), *Tshz2* (lane 2) and *Tshz3* (lane 3) mRNA DIG–labeled probes. Bars: 100 μM

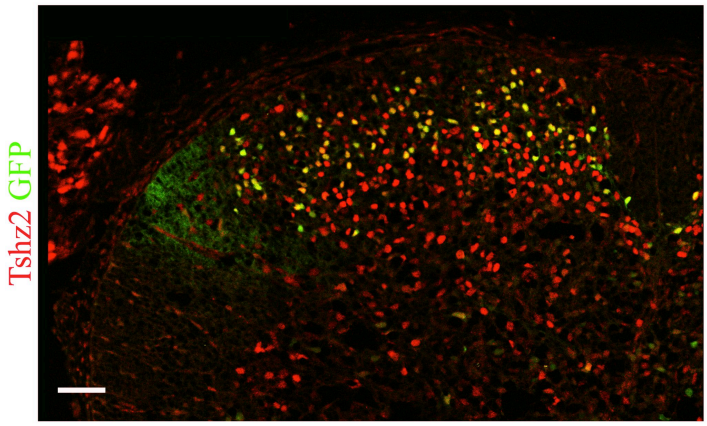

Fig.3.6. Immunostaining with anti-Tshz2 (red) and anti-GFP (green) antibodies on a transversal section of P0 spinal cord from a *Tshz1* $^{GFP/+}$ mouse. Bar: 500μm

3.3 Preliminary functional analysis of *Tshz1* in the developing spinal cord.

The *Tshz1*$^{GFP/GFP}$ mouse (see §2.1.2 for description) was used to gain insights about a possible functional relevance of *Tshz1* in the development of the spinal cord. In order to test for a regulatory activity of *Tshz1* on gene expression in the dorsal spinal cord, I performed a microarray expression analysis of E15.5 dorsal spinal cord from wild type and *Tshz1*$^{GFP/GFP}$ mice. I isolated the total RNA and processed it for hybridization on Affymetrix MOE430 2.0 microarrays, which was performed by the group of Prof. Dr. Norbert Huebner (MDC, Berlin). The comparison of expression intensity from wild type and homozygous *Tshz1*^{GFP} mice revealed just a few differentially expressed genes (see table 3.1). This could be due to redundancy amongst the three *Teashirt* genes, as suggested by the overlapping distribution of their transcripts from midgestation onwards.

To confirm the coexpression of different Teashirts, antibodies against murine Tshz1 and Tshz2 were raised in rabbit (see §2.3.6); Fig. 3.6 shows overlapping immunoreactivity of the two transcription factors in the most superficial layer of the P0 dorsal spinal cord, where most of the Tshz1+ cells coexpress Tshz2. Interestingly, the Affymetrix analysis revealed that *Tshz1* expression itself is upregulated in the *Tshz1* mutant, suggesting a negative autoregulation of the endogenous *Tshz1*.

Table3.1. Differentially expressed genes in the dorsal spinal cord of P0 *Tshz1*$^{GFP/GFP}$ mice. (FC= fold change)

Gene	Affymetrix probe	P value	FC
M-phase phosphoprotein 9	1431053_at	1.81 e-06	0.33
Regulatory factor X domain containing 2	1457847_at	5.65 e-06	8.50
Teashirt1	1446707_at	1.56 e-07	5.07
Polyadenylate binding protein-interacting protein1	1441955-s_at	1.61e-07	4.1

3.4 Analysis of *Tshz1* expression in the developing olfactory system.

Previous studies (Caubit et al., 2005) showed that the transcripts of the three murine *Teashirts* are complementarily distributed in the developing diencephalon, telencephalon and olfactory bulb. I therefore focused the functional analysis of *Tshz1* on the olfactory system, in the expectation that *Tshz1* functions would not be compensated by other *Tshz* genes. For the detailed expression analysis in the olfactory system, I studied the immunoreactivity of the reporter GFP in the *Tshz1*$^{GFP/+}$ mice, because Tshz1 and GFP showed overlapping expression (Fig.3.7).

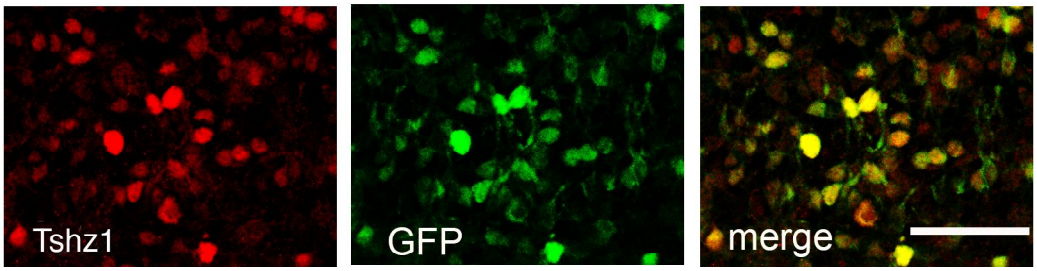

Fig.3.7. Immunostaining of the olfactory bulb granule cell layer from a P0 *Tshz1*$^{GFP/+}$ mouse showed complete overlap of Tshz1 and GFP immunoreactivity. Bar: 50 μM

3.4.1 *Tshz1* expression at E12.5

Immunohistochemistry on coronal sections of *Tshz1*$^{GFP/+}$ brains at the level of the ganglionic eminences showed strong GFP expression in the LGE mantle zone (Fig.3.8). Moreover, a thin marginal line of GFP-positive cells spread dorsally extending into the pallium. GFP expression was excluded from progenitors in the ventricular zone of the lateral ventricle, which was marked by Pax6 staining (Fig.3.8A). Some cells in the sub-ventricular zone, however, maintained Pax6 expression and partially coexpressed GFP. GFP immunoreactivity overlapped completely with Doublecortin (Dcx), a marker for immature and migrating cells, while no costaining was detected with NeuN, which is expressed exclusively by mature neurons (Fig.3.8C). Previous studies (Stenman et al., 2003) showed that the Islet1+ subpopulation of subpallial progenitors gives rise to interneurons of the striatum; as the GFP+ cells did not co-label for Islet1 (Fig.3.8C), we can conclude that *Tshz1* expressing cells don´t belong to this subpopulation of striatal progenitors.

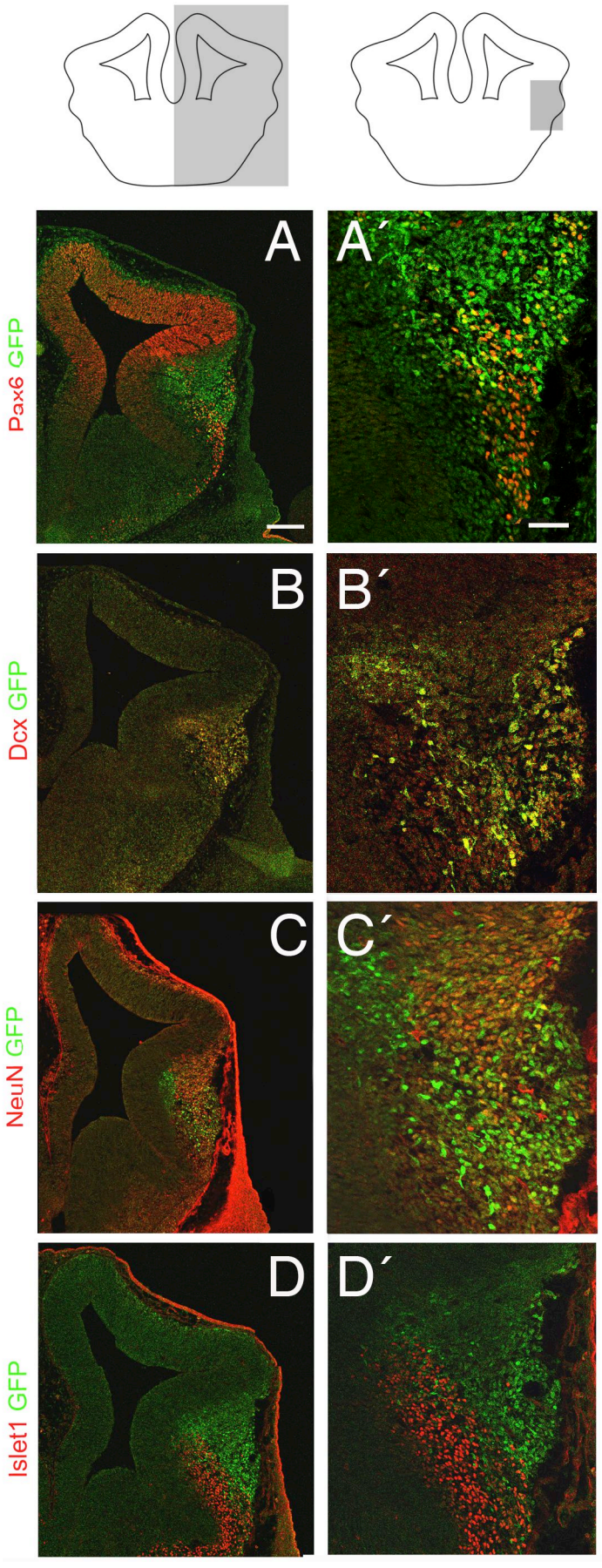

Fig.3.8. Immunohistological analysis of *Tshz1* expression in the LGE at E12.5. Coronal sections at the ganglionic eminencelevel of E12.5 brains from *Tshz1*$^{GFP/+}$ mice were stained with anti-GFP antibody (green) and costained with anti Pax6, Dcx, NeuN, Islet1 (red). Pictures in the left column are magnified on the right, and the scheme at the top identifies the region of the brain shown in the pictures. GFP was costained with post-mitotic markers for immature, migrating cells (Dcx, partially Pax6), but didn´t costain with NeuN, a marker for mature neurons, and Islet1, a marker for cells that will migrate to the striatum. Bar (in A):250 μm; Bar (in A´): 125 μm.

3.4.2 *Tshz1* expression in the E14.5 LGE

At E14.5, GFP expressing cells were spread throughout the mantle zone of the LGE (Fig.3.9); co-staining for GFP, Pax6 (marker for the pallial ventricular zone) and Mash1 (marker for the subpallial ventricular zone) (Fig.3.9A, B) identified a population of GFP+ cells localized in the sub-ventricular zone at the boundary between pallium and subpallium, in the dorso-lateral ganglionic eminence (dLGE). This specific anatomic localization spatially overlapped (but did not co-stain) with the Er81+ domain (Fig.3.9 F), which was shown to contribute to OB neurogenesis (Torresson et al., 2000; Stenman et al., 2003). On the contrary, the Isl1+ domain represents a pool of striatal progenitors and was completely excluded from GFP immunoreactivity (Fig3.9 E). Similarly to previous embryonic stages, the dLGE-located GFP+ cells coexpressed Dcx but not NeuN (Fig. 3.9 C, D), indicating that the population is entirely constituted of immature migrating cells.

3.4.3 *Tshz1* expression in the E14.5 olfactory bulb

At E14.5, the olfactory bulb (OB) starts to be populated by pioneer interneuron progenitors that derive from the LGE (Yoshihara et al., 2005). Immunohistochemistry on olfactory bulb coronal sections at this stage showed a large population of GFP+ cells at the periphery of the bulb. The GFP expressing population was excluded from the progenitor zone, situated at the core of the bulb and marked by Mash1 and Pax6 (Fig.3.10 A, B). Notice that as in the ganglionic eminence, Pax6 remained expressed in a population of postmitotic neurons, which partially co-expressed GFP.

Er81 is expressed in OB periglomerular and granule interneurons from embryonic life to adulthood; at midgestation Er81+ interneurons are already strongly detectable in the olfactory bulb, but only few of them co-expressed GFP, Er81 being expressed closer to the core of the bulb and GFP+ cells being distributed more peripherally (Fig.3.10 C). GABA expression is detected in the interneurons as they begin to mature and migrate radially to the external layers, and it is already observed at E14.5 at the periphery of the bulb (Fig. 3.10 D). All the GABA+ interneurons at this stage co-expressed GFP.

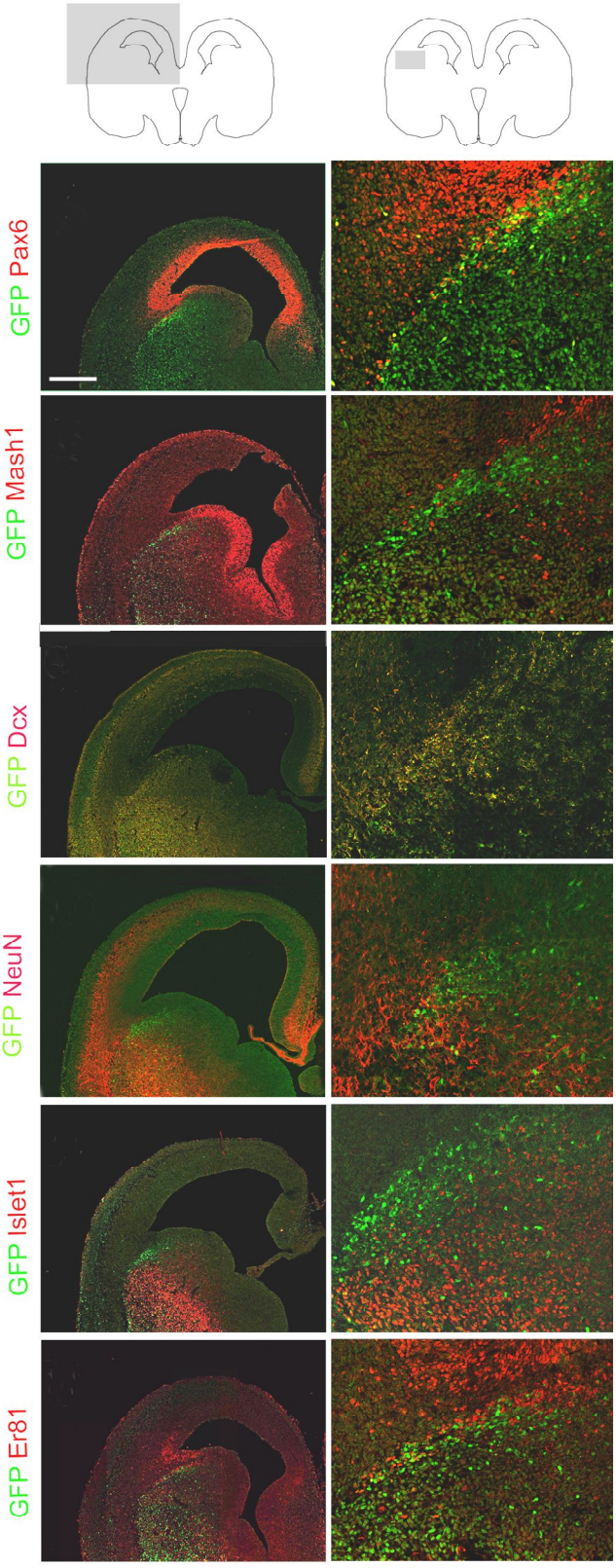

Fig.3.9. Immunohistological analysis of Tshz1 expression in E14.5 dLGE. Coronal sections of E14.5 brain from *Tshz1*$^{GFP/+}$ mice were stained with anti-GFP antibody (green) and costained with anti-Pax6, anti-Mash1, anti-Dcx, anti-NeuN, anti-Islet1, anti-Er81 antibodies (red). Pictures in the left columns are magnified in the right, as shown in the schemes on the top. GFP was partially costained with post mitotic Pax6, while no costaining with the progenitor marker Mash1 was detected. GFP expression totally overlapped with Dcx, while no costaining at this stage was detected with NeuN (marker for mature neurons), Islet1 (marker for cells migrating to the striatum), and Er81 (marking a subpopulation of interneuron progenitors that will migrate to the granule cell layer of the olfactory bulb). Bar: 500μm in A-F; 250 μm in A´-F.

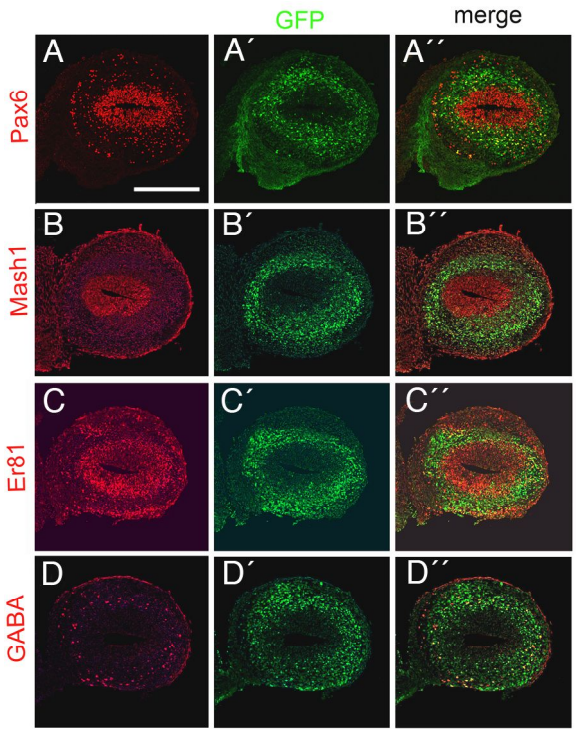

Fig.3.10. Immunohistological analysis of Tshz1 expression in E14.5 OB of *Tshz1*$^{GFP/+}$ mice. Coronal sections of E14.5 brains at the level of the OB were stained with anti-GFP antibody (green) and costained with anti-Pax6, anti-Mash1, anti-Er81 and anti-GABA (red). GFP was coexpressed in the Pax6-expressing postmitotic cells, while it was not costained with the progenitor marker Mash1. The GFP+ ring of granule cells is localized externally to the Er81+ granule cell subpopulation and overlaps just partially with it. Finally, all GABA+ interneurons at this stage coexpress GFP. Bar: 300µm.

3.4.4 *Tshz1* expression in the E14.5 rostral migratory stream

At E14.5, the rostral migratory stream (RMS), which contains the pioneer OB interneuron progenitors migrating from the dLGE to the OB primordium, is already visible (Wichterle et al., 2001), and it expresses most of the transcription factors marking OB interneurons (such as Er81, Dlx5/6, Arx and Sp8). As Tshz1 is expressed by cell populations in the dLGE and in the OB, I analysed whether migrating progenitors in the RMS maintain Tshz1 expression by immunostaining of parasagittal sections from E14.5 *Tshz1*$^{GFP/+}$ brains with anti-GFP and anti-Pax6 antibodies (Fig.3.11). A population of GFP+ postmitotic cells extended from the LGE to the OB along the RMS visualized by Pax6 expression. However, Pax6 and GFP were not co-expressed by the cells in the stream.

I further visualized the GFP+ cells in the RMS by GFP and Er81 immunostaining in a series of coronal sections, starting at the bulb and proceeding caudally till the ganglionic eminecences. Fig.3.12 shows four coronal planes, taken at the levels indicated in the scheme shown above. The drawings on the left side of every picture (from Long et al., 2007) visualize schematically the anatomical location of the stream (including a central progenitor domain and a peripheral postmitotic domain) at every level. Progenitors coming from the pallium are indicated in red, progenitors coming from the subpallium are indicated in green. In the immunostainings, Er81 expression (red) was used to mark the RMS at every level of section. Note that Er81 was always expressed, as expected, in the SVZ of the subpallial domain. Within the bulb, GFP (green) and Er81 marked two different subpopulations, as already described (Fig.3.9C). Caudally to the bulb, in zones III and IV, GFP expression partially overlapped with Er81 expression in the SVZ of the subpallial domain (fig3.12 arrows), showing that the *Tshz1*+ cells populate the RMS.

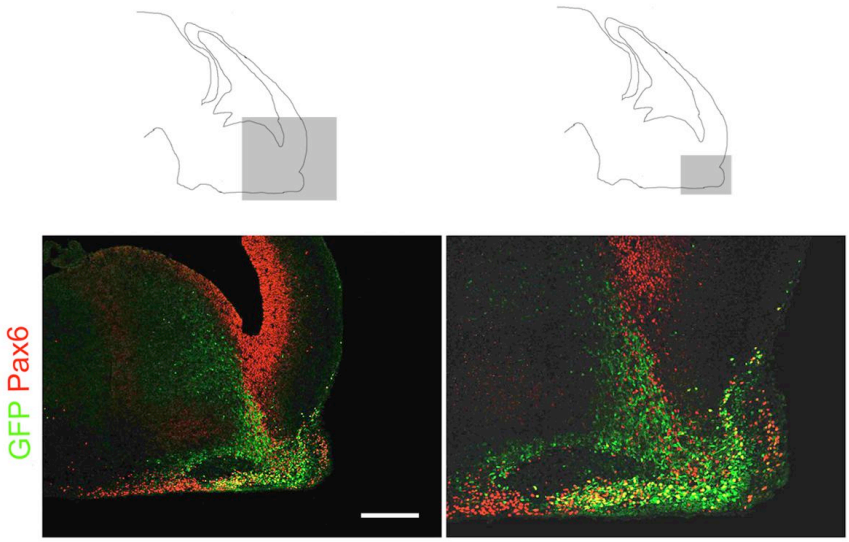

Fig.3.11. Expression of *Tshz1* in the rostral migratory stream at E14.5. Sagittal section of brain from E14.5 *Tshz1*$^{GFP/+}$ embryo immunostained with anti-GFP (green) and anti-Pax6 (red) antibodies. GFP expression is detected in the Pax6 negative postmitotic cells along the RMS from the LGE to the OB. At the level of the OB, partial GFP/Pax6 costaining is detected.The right panel is a magnification of the left one. Bar. 500μm left, 250μm right panel.

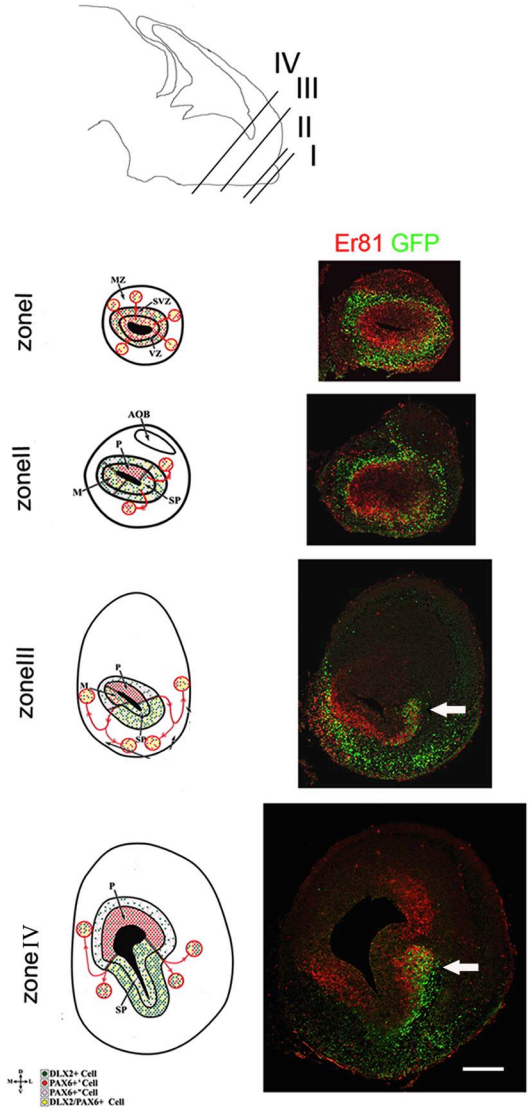

Fig.3.12. A series of coronal sections starting from the OB level and proceeding caudally was costained with anti-GFP (green) and anti-Er81 (red) antibodies. The scheme at the top shows the levels where the four coronal sections were taken.The drawings at the left side of every picture show the localization of the progenitor and postmitotic populations of the RMS at each level (Long et al., 2007). GFP was expressed throughout the series in the postmitotic region of the RMS, marked by Er81 expression. MZ: mantle zone; SVZ: subventricular zone; VZ: ventricular zone; AOB: accessory olfactory bulb; P. pallial domain; SP: subpallial domain; M: mixed domain. Bar: 300μm.

3.4.5 *Tshz1* expression at P0

At P0, the anatomical layering of the bulb is clearly defined; GFP was strongly expressed in the outer ring of the granule cell layer, and few GFP positive cells were scattered in the glomerular cell layer (Fig.3.13). At this stage, the inhibitory neurotransmitter GABA is synthesized by granule cells and periglomerular interneurons, and its immunoreactivity in the outer ring of the granule cell layer completely overlaps with GFP (Fig.3.13 A). Also the few GFP+ periglomerular

interneurons express GABA. Tyrosine hydroxylase marks a subset of GABAergic interneurons and co-stained completely with GFP in the granule cells but not in the periglomerular cells (Fig.3.13 B). Immunostaining with anti-GFP and anti-Tshz2 antibodies showed that the two *Teashirt* genes have complementary expression in the layers of the bulb: Tshz1 was expressed in the granule cells and periglomerular layer and Tshz2 just in the mitral cell layer (Fig. 3.13C). At the level of the lateral ventricle, GFP was still strongly expressed at P0 (Fig. 3.14); at this stage, GFP expressing cells were excluded from the Pax6+ progenitor domain. However, GFP and NeuN did not co-stain, indicating that cells expressing GFP are postmitotic but immature.

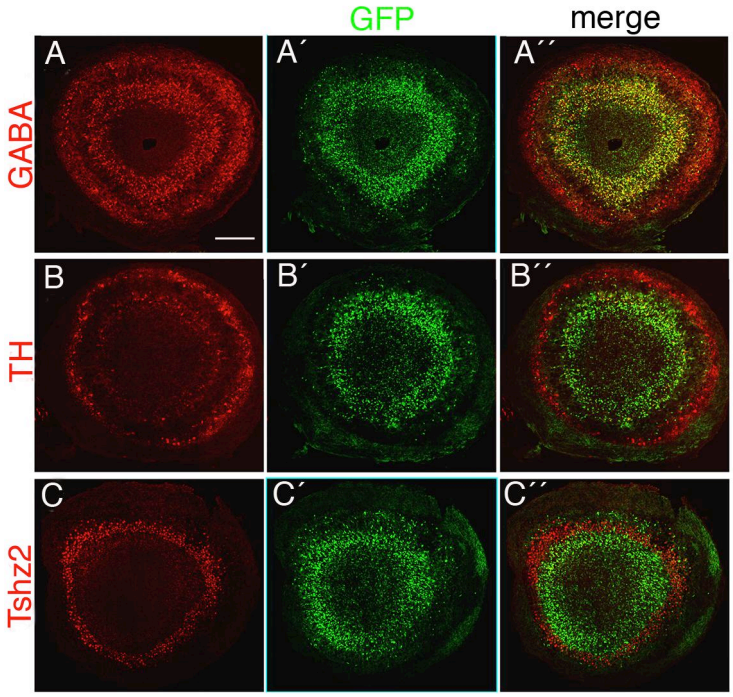

Fig.3.13. Immunohistological analysis of *Tshz1* expression in the OB at P0. Brains from *Tshz1*$^{GFP/+}$ pups were sectioned at OB level, immunostained with anti-GFP antibody (green) and with anti-GABA, anti-TH, anti-Tshz2 (red).GFP is coexpressed in the granule layer with GABA and TH but not with Tshz2 (marker for mitral cells). Bar. 500µm.

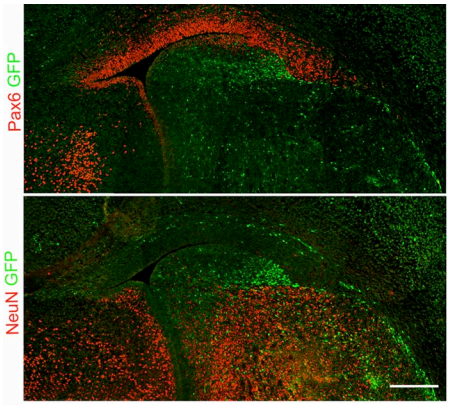

Fig. 3.14. Tshz1 expression in the subventricular zone at P0. Coronal sections of P0 brains at the level of the lateral ventricle were stained with anti-GFP (green) and costained with anti-Pax6 and anti-NeuN antibodies (red). GFP immunoreactivity is maintained in the postnatal subventricular zone. Bar: 500µm

3.4.6 *Tshz1* expression at P18

During adulthood, GFP immunostaining was strongly detected in granule and periglomerular cells, showing that the gene is a specific marker for OB interneurons from early development to adulthood, consistent with a dLGE/SVZ origin of *Tshz1*+ interneurons (Fig.3.15).

At least three distinct populations of OB interneurons can be identified by the expression of the calcium-binding proteins, calbindin and calretinin, or the production of GABA. GFP+ cells co-expressed both GABA and calretinin in granule and periglomerular layers (Fig.3.15). Specifically, GFP+ and calretinin+ subpopulation completely overlapped in the periglomerular layer (fig.3.15 F). Notice that a large GFP+ domain closer to the core of the bulb expressed neither of the two markers and it consists probably of immature granule cells. Interestingly, GFP and Tshz2 immunoreactivity partially overlapped in the periglomerular layer, although they were complementary in the other layers of the bulb (Fig.3.15).

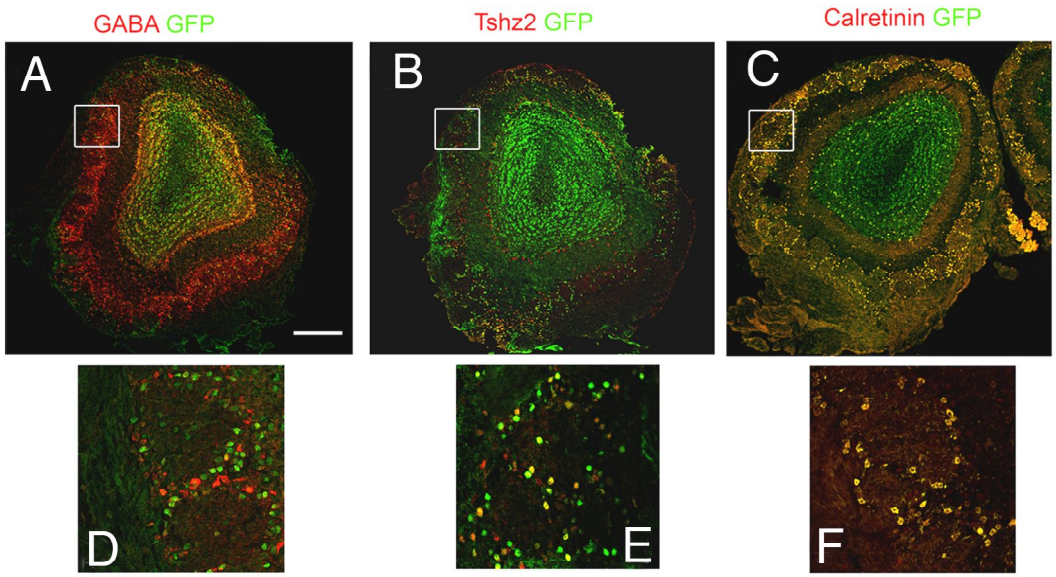

Fig.3.15. Analysis of Tshz1 expression in P18 OB. Immunostaining of coronal sections of OB from P18 *Tshz1*$^{GFP/+}$ mice. The sections were costained with anti-GFP (green) and anti-GABA (A, D), anti-Tshz2 (B, E) and anti-calretinin (C, F) antibodies respectively (red). In mature OB, GFP is strongly expressed in granule and periglomerular cells. GFP and calretinin expression completely overlap in the periglomerular neurons. No expression of Tshz1 is detected in the mitral cells. Inserts are magnifications of the upper panels. Bar in A represents 1000μm in A,B,C and 250μm in D,E,F.

3.5 *Tshz1* deletion results in olfactory bulb granule cells defects.

Characterization of *Tshz1* expression in the developing olfactory system revealed that the transcription factor is strongly expressed from E12.5 to adulthood and that *Tshz1* and *Tshz2* expressions domains in the olfactory bulb are complementary and do not overlap at any stage of development. Therefore, to gain insights into *Tshz1* functions in the developing olfactory system and in particular during OB interneuron generation, I analyzed the olfactory bulb organization in mutant *Tshz1*$^{GFP/GFP}$ mice, in which the *Tshz1* coding sequence was disrupted by insertion of a GFP reporter cassette (see § 3.1.2). Because of the lethality of the *Tshz1* mutation, analysis of adult mice is not possible at the moment, and will be therefore performed in *Tshz1* conditional mutants after the establishment of the strain (see § 3.1.2).

I started my investigation by comparing olfactory bulbs from *Tshz1*$^{GFP/+}$ and *Tshz1*$^{GFP/GFP}$ animals at stage P0, when the layered structure is clearly detectable even though the bulb is not completely mature. Coronal sections of the olfactory bulbs were hybridized with a DIG-labelled *Reelin* probe, to visualize mitral cells (Fig. 3.17 A, B). *Reelin* expression appeared unchanged in the mutant tissue, as could be expected from the fact that the mitral layer only expresses *Tshz2*.

GAD67 (GAD1), Glutamic acid decarboxylase 67, is an enzyme required for GABA synthesis and therefore marks GABAergic cells. Glutamic acid decarboxylase exists also in a second form, called GAD65; the two forms were shown to be encoded by two different genes (Erlander et al., 1991; Bu et al., 1992) and to be differentially distributed in the CNS (Esclapez et al., 1993). Different levels of expression of the two *GAD* genes in different groups of GABAergic neurons may be related to differences in the functional properties of the neurons. I analyzed therefore the relative distribution of *GAD67* and *GAD65* mRNAs in the wild type olfactory bulb granule cell layer. The double in situ hybridization experiment pictured in Fig.3.16 shows that at P0 the two genes have complementary expression domains, *GAD65* mRNA being mainly distributed in the core region and *GAD67* in the outer region of the granule cell layer, which corresponds to the *Tshz1* expression domain. Thus, I analyzed whether and how loss of *Tshz1* affects the two populations of granule cells

marked by GAD67 and GAD65 using in situ hybridization on coronal sections of P0 olfactory bulbs.

In the *Tshz1* mutant olfactory bulb, *GAD67* mRNA is lost specifically in the outer ring of the granule cell layer, while in the glomerular layer, *GAD67* expression remains unchanged (Fig.3.17 C, D, arrows). This indicates that *Tshz1* is specifically essential for the correct development of the GAD67 positive neuronal subtype in the outer granule cell layer. I addressed the question whether *Tshz1* is required also for the development of *GAD65* positive GABAergic granule cells by comparing the distribution of *GAD65* mRNA in control and mutant olfactory bulbs (Fig3.17 E, F). The experiment showed that loss of *Tshz1* results in an enhancement of *GAD65* expression in the outer ring of the granule cell layer (arrows).

I further analyzed the mutant phenotype using immunohistochemistry. A first piece of information could be obtained from the comparison of GFP expression in control and mutant mice (Fig.3.17 G-N, green). In the *Tshz1*$^{GFP/GFP}$ OB, the concentration of the GFP+ interneurons in the external ring of the granule cell layer as observed in the *Tshz1*$^{GFP/+}$ mice is lost, and GFP expressing cells are widely distributed throughout the granule cell layer, with some areas of higher GFP+ cell density. This suggests a defect in the radial distribution of *Tshz1*+ neurons coming from the RMS and migrating to the external layers of the bulb.

Immunostainings on coronal sections of P0 wild type and mutant olfactory bulbs indicated that the synthesis of GABA in the outer granule cells is completely lost in the absence of *Thsz1*. On the contrary, GABA immunoreactivity remains unchanged in the mutant periglomerular interneurons (Fig.3.17, G, H). Another subset of OB interneurons is marked by tyrosine hydroxylase (TH), the rate-limiting enzyme in dopamine production. As all the TH immunopositive granule co-express Tshz1 at P0 (Fig.3.13 B), I analyzed whether loss of *Tshz1* affects their correct development. Immunostaining of mutant olfactory bulbs with anti TH antibody showed that mutation of *Tshz1* led to the loss of the TH+ granule cell subpopulation but did not affect expression of TH in periglomerular interneurons. I finally verified whether *Tshz1* affects *Tshz2* expression. Immunostainings of control and mutant OB with Tshz2 antibody showed that *Tshz2* expression remains unchanged (Fig.3.17 I, L).

I could therefore conclude from these data that *Tshz1* is necessary for the correct establishment of the subset of granule cells that populate the outer ring of the granule cell layer at P0. The absence of *Tshz1* provokes a striking phenotype at the level of the granule cell layer without affecting periglomerular interneurons and mitral cells. Future studies in adult conditional mutants will clarify if *Tshz1* and *Tsh2* have a role in the renewal of the periglomerular interneurons, which is suggested by their strong expression in this layer during adulthood.

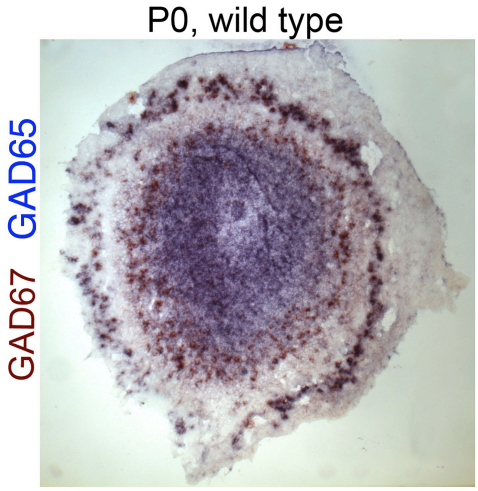

Fig 3.16. Differential distribution of *GAD65* and *GAD67* mRNAs in the granule cell layer. Double in situ-hybridization on a coronal section from P0 wild type OB. DIG-labeled *GAD65* (blue) and FITC-labeled *GAD67* (red) mRNA probes were used. *GAD65* mRNA is mainly concentrated at the core of the granule cell layer, while *GAD67* is strongly expressed in the outer ring, which corresponds to the Tshz1+/GABA+ granule cell subset.

Fig 3.17. Granule cell defects in P0 *Tsh1*$^{GFP/GFP}$ mice. (A-F) in situ-hybridization on coronal sections of P0 *Tshz1*$^{GFP/+}$ and *Tshz1*$^{GFP/GFP}$ mouse OB with *reelin* (A, B) , *GAD67* (C, D) and *GAD65* (E, F) DIG-labeled probes. The *GAD67* signal in the outer granule cell layer was lost in the mutant, while it remained unchanged in the glomerular layer (arrows). The *GAD65* signal in the mutant was expanded to the outer ring of the granule cell layer. The reelin expression in the mitral cell layer remained unchanged in the mutant. (G-N) Immunohistochemistry on coronal sections of P0 *Tshz1*$^{GFP/+}$ and *Tshz1*$^{GFP/GFP}$ mouse OB. The sections were stained with anti-GFP (green) and anti-GABA (red, G, H), anti-TH (red, I, L), and anti-*Tshz2* (red, M, N) antibodies. GABA+ and TH+ granule cell subpopulations are lost in the mutant. *Tshz2* expression remains unchanged in the mutant OB. Note abnormal distribution of GFP+ cells in the mutant. Bar: 500μm.

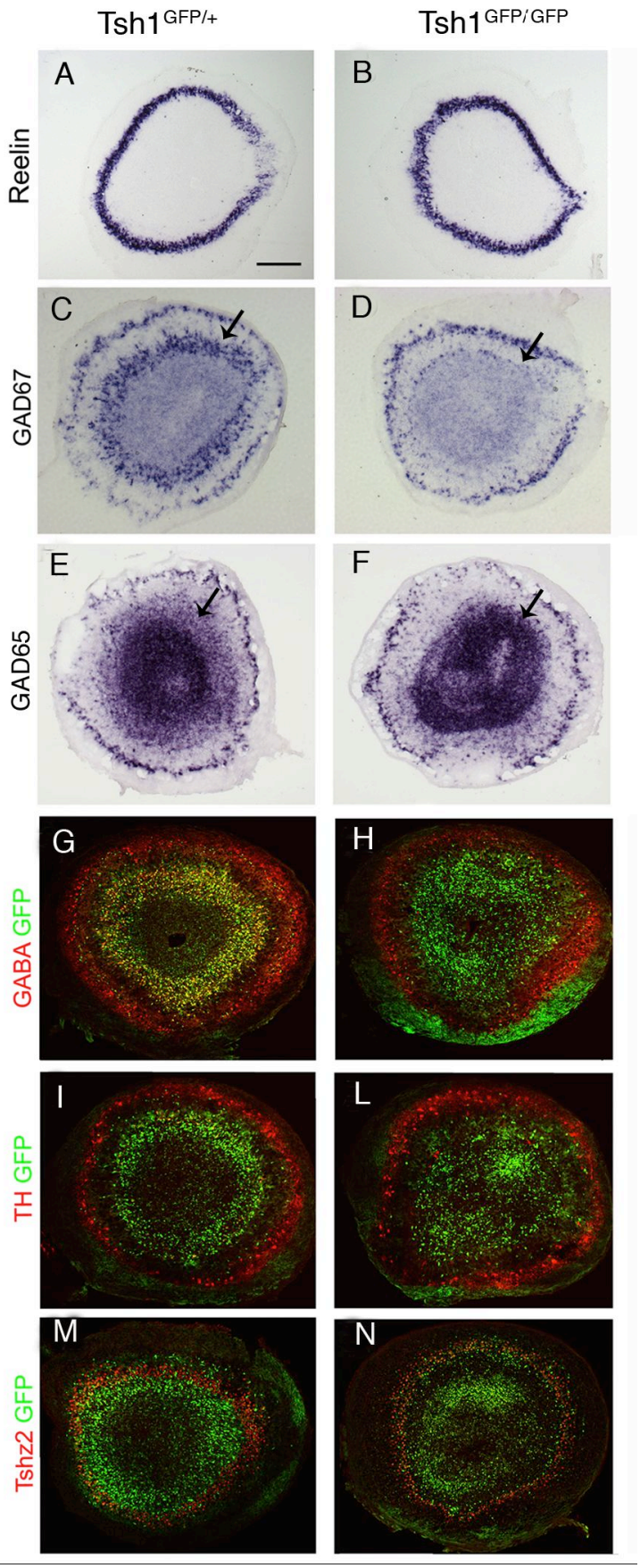
Tsh1GFP/+
Tsh1GFP/GFP
A
B
Reelin
C
D
GAD67
E
F
GAD65
G
H
GABA GFP
I
L
TH GFP
M
N
Tshz2 GFP

3.6 Characterization of the GFP+ cells in *Tshz1* mutant OB

After reaching the OB through tangential migration, the immature interneurons change orientation to migrate radially and populate the granule cell and periglomerular layers. They then further differentiate into local circuit neurons. Hardly anything is known so far about the regulation of this last part of interneuron differentiation. The distribution of GFP+ cells in the *Tshz1*$^{GFP/GFP}$ OB suggested a deficit in their radial migration. Therefore, characterization of the aggregated GFP+ cells could provide insights about the mechanisms underlying the final differentiation of interneuron precursors. Specifically, I addressed the question whether the GFP+ cells of control and mutant OB differ only in spatial distribution or also in their differentiation state by costaining coronal sections from P0 OB with anti-GFP antibody and different postmitotic markers (Fig.3.18). I first analyzed the co-expression of GFP and Pax6; as already shown, most proliferating SVZ progenitors express the transcription factor Pax6, but only a small subpopulation of migrating neuroblasts and new olfactory bulb interneurons retain Pax6 expression (Fig. 3.8A, 3.9A, 3.10A). In the olfactory bulb at P0, some of the Pax6+ postmitotic neurons that populate the granule cell layer and the glomerular layer expressed GFP; however, GFP at this stage marked a much larger population of granule cells than Pax6 and the majority of GFP+ cells did not express Pax6 (Fig.3.18A). In the *Tshz1*$^{GFP/GFP}$ OB, the partial co-expression of GFP and Pax6 was maintained, and a small number of Pax6+/GFP+ cells were detectable. The distribution of Pax6+ granule cells in the mutant was altered as compared to the control and resembled the aggregated pattern of the GFP+ cells.

Doublecortin (Dcx) is a microtubule-associated phosphoprotein required for normal neuronal migration in the developing brain, where it is widely expressed in both radially and tangentially migrating neuroblasts of cortex, RMS and OB. As already shown (Fig. 3.8B, Fig.3.9 C), Dcx immunoreactive cells in the developing SVZ correspond to the GFP+ subpopulation of immature interneurons. Similarly, in the P0 OB, Dcx and GFP immunoreactivity completely overlapped (Fig. 3.18 C). This distribution of Dcx in the granule cell layer is in agreement with previous findings (Nacher et al., 2001) that Dcx is expressed not only by migrating undifferentiated

interneurons, but also by newly differentiated interneurons of OB, piriform cortex and dentate gyrus. After disruption of *Tshz1*, the irregularly distributed GFP+ cells maintain Dcx expression (Fig. 3.18 D).

Calretinin (CR), a calcium binding protein expressed by a subpopulation of GABAergic granule and periglomerular interneurons, is expressed in the control P0 OB by many, but not all GFP immunoreactive granule cells (Fig. 3.18 E). Surprisingly, although the GFP+ neurons lose GABA and TH expression in the absence of *Tshz1* (Fig. 3.17 G-L), they maintain calretinin immunoreactivity (Fig. 3.18 F). In the absence of *Tshz1*, therefore, the GFP+ population loses just some of the postmitotic markers expressed in the control (GABA, TH, GAD67), while the expression of others (Dcx, Pax6, CR, GAD65) is maintained. Thus, I addressed the question whether loss of *Tshz1* results in maturity deficit of granule cells, by analyzing the expression of NeuN, a marker expressed exclusively by mature neurons, in the control and mutant olfactory bulb. At P0, NeuN marks few periglomerular neurons as well as the outer ring of the granule cell layer, where its immunoreactivity largely overlaps with GFP (Fig. 3.18 G). However, *Tshz1* deletion leads to a loss of NeuN expression in GFP+ cells, meaning that the gene is essential not only for the radial migration, but also for the maturation of granule cell (Fig. 3.18 H).

Finally, I tested whether in the *Tshz1* mutant olfactory bulb the irregularly distributed, immature GFP+ cells are mis-specified. Er81 is a marker for granule cells from embryonic life to adulthood, and at P0 it marks the inner granule cell layer but it is excluded from the *Tshz1* positive outer ring, indicating that the two transcription factors mark different granule cell subpopulations (Fig. 3.18 I), in agreement with the lack of co-expression already observed at E14.5 both in the LGE (Fig. 3.9 F) and in the bulb (Fig. 3.10 C). In the *Tshz1*$^{GFP/GFP}$ mouse, the aggregated GFP+ cells did not co-express Er81, suggesting that loss of *Tshz1* does not lead to a fate shift between different subpopulations of granule cell interneurons.

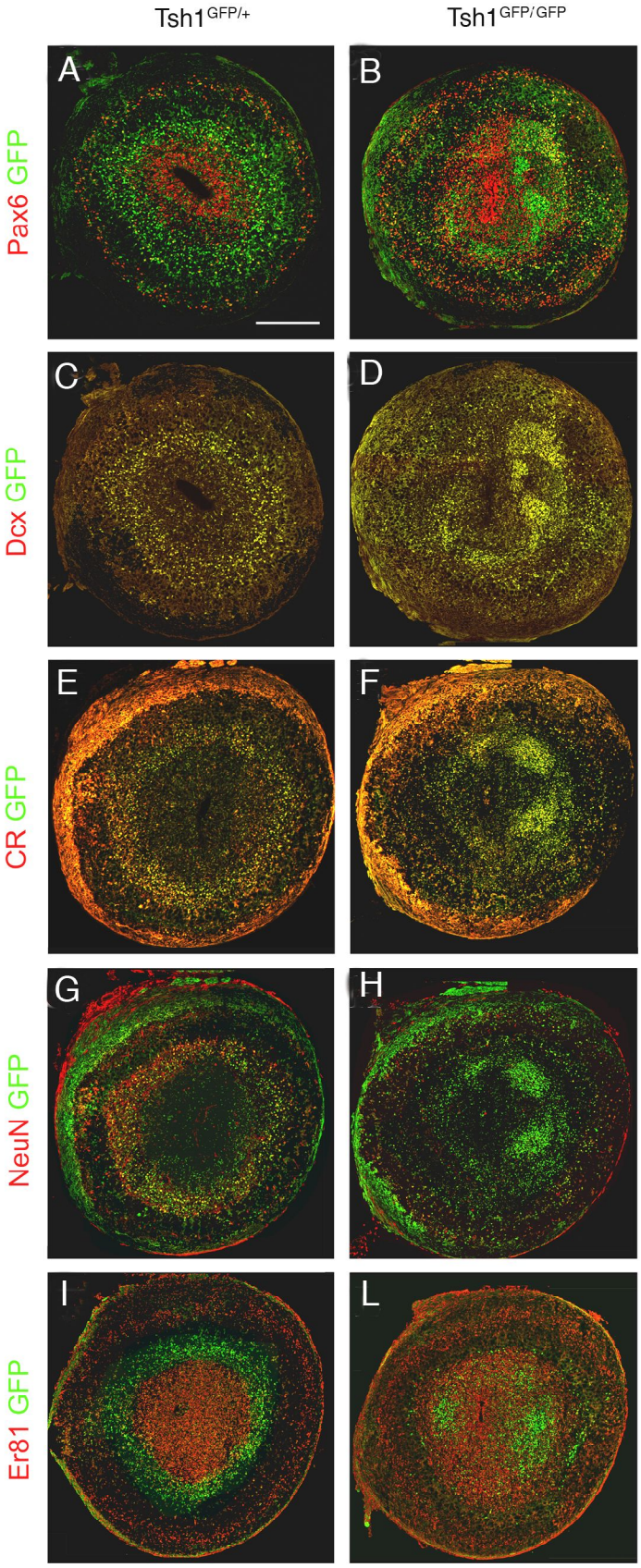

Fig.3.18. Characterization of the GFP+ cells in the olfactory bulb of *Tshz1* mutants. Coronal sections of P0 olfactory bulbs of *Tshz1*$^{GFP/+}$ (A, C, E, G, I) and *Tshz1*$^{GFP/GFP}$ (B, D, F, H, L) mice were stained with anti GFP (green) and anti-Pax6 (A, B), anti-Dcx (C, D), anti-Calretinin (CR) (E, F), anti-NeuN (G, H) and anti Er81 (I, L) antibodies (red).
Pax6 and GFP are partially coexpressed both in control and mutant. Total overlap of GFP and Dcx expression is detected in the control as well as in the mutant. Also Calreinin/GFP coexpression is maintained in the mutant olfactory bulb. NeuN is coexpressed with GFP in the control but not in the mutant mouse. Finally, GFP+ cells do not coexpress Er81, neither in the control nor in the mutant. Bar: 500μm

3.7 Genesis of the *Tshz1* positive granule cell subpopulation.

The production, migration and differentiation of the earliest generated OB interneurons are largely unexplored. Previous studies showed that OB interneuron precursors are specified in the LGE between E12.5 and E14.5, and that they give rise to a heterogeneous population of stable OB interneurons, but no birth dating studies about the distinct subpopulations were described (Tucker et al, 2006).

In order to identify the precise time window in which the *Tshz1* dependent subset of granule cells is generated, I used BrdU pulse/chase labelling in wild type mice. BrdU was injected at different times of gestation (E16.5, E14.5, E12.5, E11.5), and the injected mice were sacrificed and analyzed at E18.5. Immunofluorescence on olfactory bulb coronal sections was used to identify and quantify BrdU+/GABA+ cells, as at this stage Tshz1 expression overlaps with GABA synthesis in the outer ring of the granule cell layer (Fig. 3.19). Interestingly, the density and distribution of BrdU+ cells in the E18.5 olfactory bulb depends strongly on the day of injection. Cells that had undergone DNA synthesis after E16.5 were more densely packed in the central region of the bulb (Fig.3.19A), while cells BrdU labelled after E14.5 were dispersed throughout the granule cell layer (Fig.3.19B), indicating that these include cells that are already more mature and started to undergo the radial migration from the core to the periphery of the bulb. However, only few GABA+/BrdU+ cells were detectable when BrdU was injected at E14.5 (Fig. 3.19,G-G´-G´). When the interneurons were labelled by BrdU injection at E12.5, the density of BrdU+ cells in the core of the E18.5 bulb was decreased, and BrdU+ cells were predominantly located in the outer GABA+ granule cell layer (Fig.3.19C); BrdU and GABA immunoreactivity in the cells of the outer granule cell layer extensively overlapped (Fig.3.19 F-F´-F´). By injection at E11.5, BrdU still marked the outer cells of the granule cell layer, but its detection was stronger further outward, in the mitral cells (Fig3.19D, E-E´-E´´). Thus, GABA+ and *Tshz1*+ cells forming the outer ring of the granule cell layer at birth underwent their last cell division around E12.5, and before E14.5.

These results are in accordance with those of Tucker and colleagues (2006). Quantitative analysis confirmed that 56,3% and 66,0% of the GABA+ cells co-stain

for BrdU when BrdU is injected at E12.5 and E11.5 respectively, while just 24,1% are double positive for injection at E14.5 and 3,3% for injection at E16.5.
In conclusion, BrdU pulse/chase analysis revealed that the pioneer granule cell population that is born around E12.0 and that has reached maturity by E18.5, i.e. expresses GABA and GAD67 at this stage, depends on *Tshz1* for its correct development. It should be noted that BrdU injections at the early stages label also neurons generated from endogenous olfactory bulb precursor cells, and not only the neurons that proliferate in the LGE and reach the bulb through the RMS (Vergaño-Vera et al., 2006).

3.8 Interneuron precursors are born correctly but fail to distribute radially in the *Tshz1*$^{GFP/GFP}$ olfactory bulb

In order to analyze whether the irregularly distributed GFP+ cells in the *Tshz1* mutant are generated at the correct time point, I compared the position and distribution of the Tshz1+ precursors in the E18.5 control and mutant OB, through BrdU pulse/chase labelling. BrdU was injected at E12.0, when the majority of the *Tshz1* dependent granule cells are generated, and double immunohistochemistry on OB coronal sections was used to identify BrdU+/GFP+ cells (Fig.3.20). In the control, BrdU immunoreactivity marked periglomerular neurons, mitral cells and the outer granule cell layer, where the immunoreactivity overlapped with GFP (Fig.3.20, upper panels).
In *Tshz1* mutant, the majority of GFP+ cells were still BrdU immunoreactive, indicating that they were generated at the correct time point during development (Fig.3.20, lower panels). The BrdU+/GFP+ cells in the mutant are no longer localized in the outer granule cell layer, but irregularly distributed, indicating that they fail to distribute radially and to form the granule cell layer. Thus, *Tshz1* is not required for the correct generation of the cells that form the outer granule cell layer at E18.5, but only for their correct radial distribution.

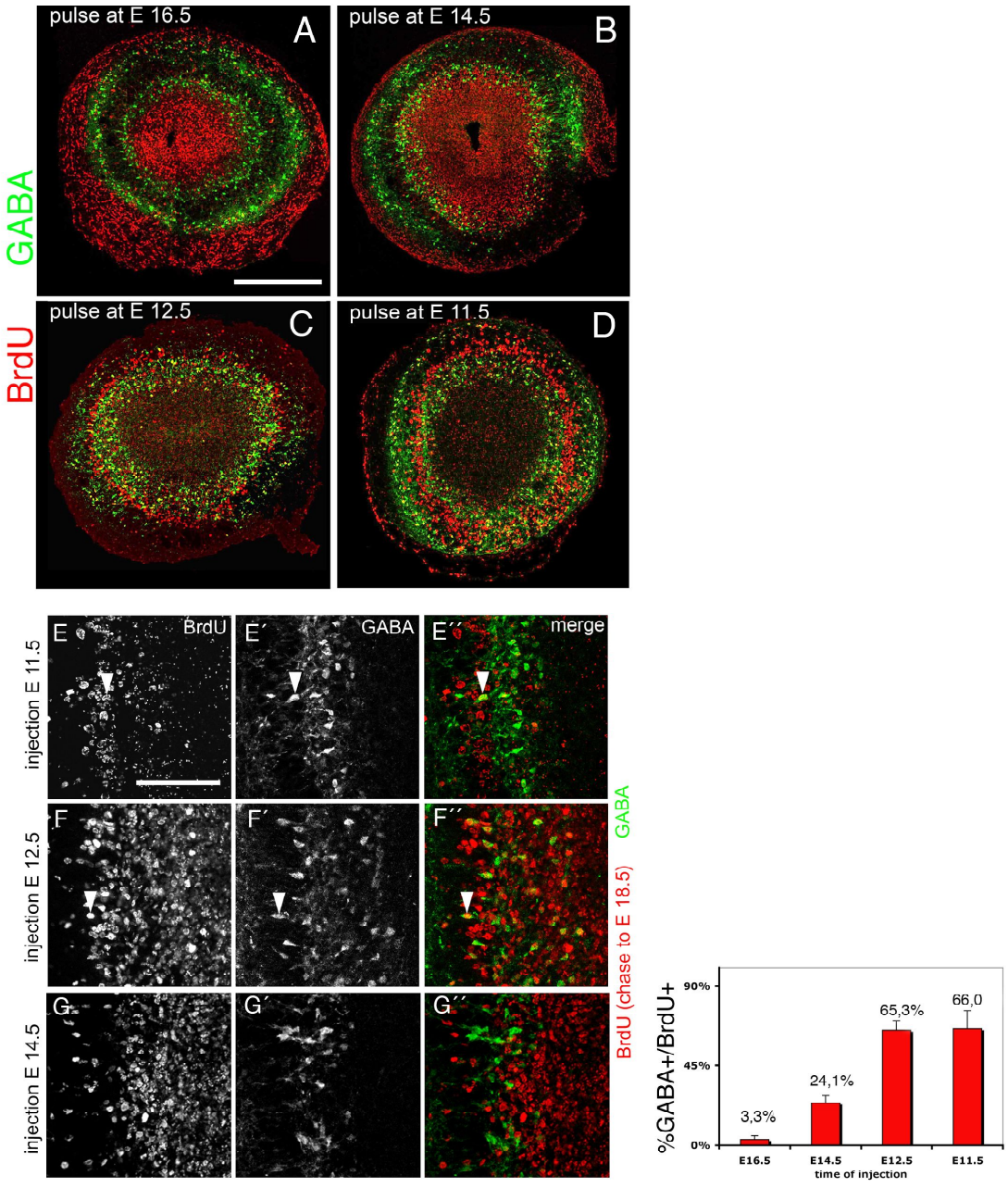

Fig.3.19. Birth dating experiment of the *Tshz1* positive granule cell population. Upper panel: immunostaining with anti-GABA (green) and anti-BrdU (red) of coronal sections from E18.5 *Tshz1*$^{GFP/+}$ mice, injected with BrdU at the different embryonic stages indicated. The majority of the GABAergic granule cells are costained with BrdU when BrdU is injected at E11.5 or E12.5. Lower panel: magnification of the GABAergic granule cell subpopulation. Graph: quantitative analysis of the percentage of the BrdU/GABA double positive cells over the total GABA positive granule cells. n=2 (inj. E16.5), n=3 (inj E14.5, E12.5, E11.5). Bar: 500μm upper panels, 200μm lower panels.

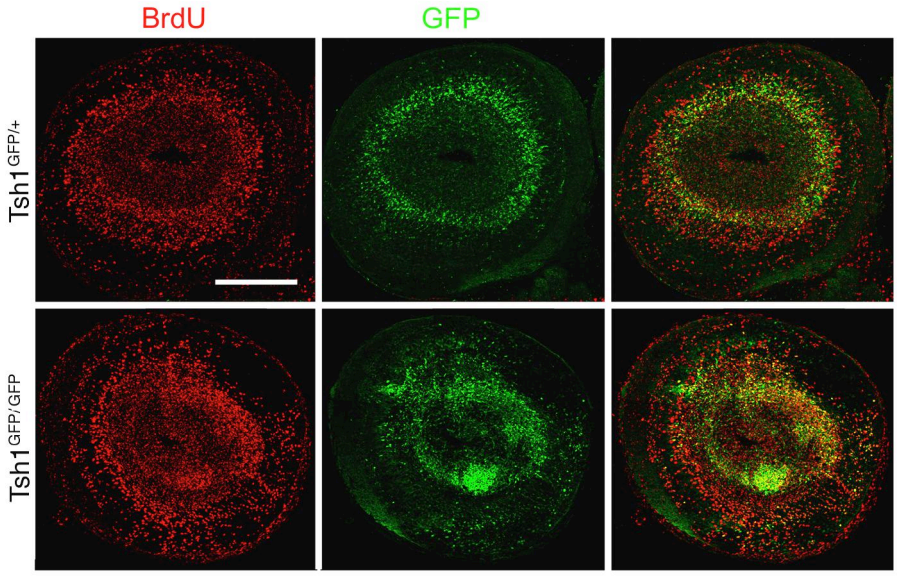

Fig.3.20. Coronal sections of olfactory bulbs from E18.5 *Tshz1*$^{GFP/+}$ and *Tshz1*$^{GFP/GFP}$ mice that were BrdU injected at E12.0 were immunostained with anti-BrdU (red) and anti-GFP (green) antibodies. In the control, BrdU immunoreactivity marks the GFP+ cells in the external granule cell layer. In the mutant, BrdU still marks the majority of the irregularly distributed GFP+ cells. Bar: 500μm.

3.9 Genome wide expression analysis in the olfactory bulb of *Tshz1* mutant mice

In order to gain insights into the molecular mechanisms underlying the *Tshz1* phenotype, I performed genome wide expression analysis of olfactory bulbs from wild type and *Tshz1*$^{GFP/GFP}$ mice at P0. For this, I isolated the total RNA and processed it for the hybridization on Affymetrix MOE430 2.0 microarrays, which was performed in the group of Prof. Dr. Norbert Huebner. The comparison of expression intensities from wild type and homozygous *Tshz1*^{GFP} mice identified surprisingly only two genes, for which the level of transcripts in the mutant was significantly different ($p < 0.05$) when compared with the wild type.

Gene	Affymetrix probe	P value	FC
Semaphorin 3C	1429348_at	1.18 e-06	0.14
Cypin (guanine deaminase)	AW911807	2.72 e-06	0.27

The reason why genes such as GAD67 are not shown as significantly changed might be that their level of expression remains unchanged in the periglomerular layer of control and mutant, and therefore the decrease in the outer ring of the granule cell

layer is not sufficient to be considered significant by the quantitative algorithm. The results were verified by in situ hybridization. For this, DIG labelled mRNA probes for Sema3c and Cypin were hybridized to coronal sections from OB of P0 wild type and *Tshz1*$^{GFP/GFP}$ mice. The results shown in Fig. 3.21 confirm the down regulation of both genes in the absence of *Tshz1*. The regulation of expression of the guidance molecule Sema3C and one of its putative signalling mediating molecules, Cypin, by *Tshz1* could provide a molecular mechanism for the function of *Tshz1* in the radial migration of granule cells in the olfactory bulb.

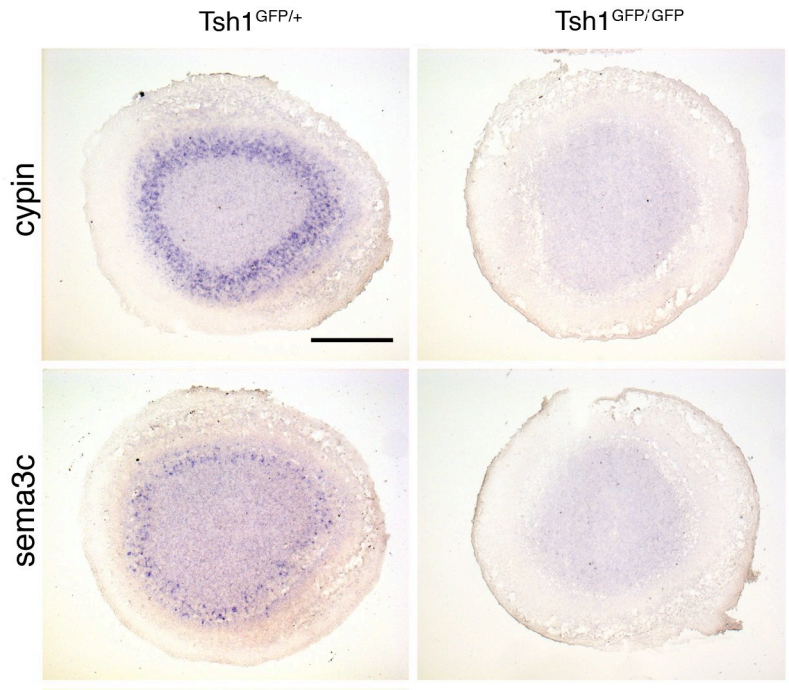

Fig 3.21. Confirmation of the Affymetrix analysis of P0 control and mutant OB. In situ-hybridization of coronal sections from P0 control and *Tshz1* mutant mice with cypin (upper panels) and Sema3c (lower panels) DIG-labelled probes. Both transcripts are lost in the mutant. Bar:500μm